Overview of the FTU results

G. Pucella[1], on behalf of FTU Team[*] and Collaborators[**]

[1]ENEA, Fusion and Nuclear Safety Department, C.R. Frascati, Via E. Fermi 45, 00044 Frascati (Roma), Italy
E-mail contact of main author: gianluca.pucella@enea.it

Abstract. Since the 2016 IAEA-FEC Conference, FTU operations have been mainly devoted to experiments on runaway electrons and investigations about a tin liquid limiter; other experiments have involved the elongated plasmas and dust studies. The tearing mode onset in the high density regime has been studied by means of the linear resistive code MARS and the highly collisional regimes have been investigated. New diagnostics, such as a Runaway Electron Imaging Spectroscopy system for in-flight runaways studies and a triple Cherenkov probe for the measurement of escaping electrons, have been successfully installed and tested, and new capabilities of the Collective Thomson Scattering and the Laser Induced Breakdown Spectroscopy diagnostics have been explored.

1. Introduction

FTU is a compact high magnetic field machine (toroidal magnetic field B_T up to 8 T, plasma current I_p up to 1.6 MA) with circular poloidal cross-section (major radius $R_0 = 0.935$ m, minor radius $a = 0.30$ m) and metallic first wall [1]. The stainless steel vacuum chamber has a thickness of 2 mm and is covered internally by a toroidal limiter made of 2 cm thick molybdenum tiles, and an outer molybdenum poloidal limiter is also present. In order to reduce the oxygen content, FTU walls are conditioned with boron coating at the beginning of any experimental campaign. Since the 2016 IAEA Fusion Energy Conference in Kyoto, FTU operations were largely devoted to experiments on runaway electrons and liquid metal limiters. Other experiments have involved the elongated plasmas, dust studies, the tearing mode onset in the high density regime and the highly collisional regimes. New diagnostics have been successfully installed and tested, and new capabilities of previously installed diagnostics have been explored.

2. Runaway Electrons studies

Post-disruption runaway electrons (RE) beam mitigation is one of the main concerns for ITER operations. RE beam control algorithms (Tore-Supra [2], DIII-D [3], FTU [4] and TCV [5]) for stabilization and current reduction can be combined with Shattered Pellet Injection (SPI) and Massive Gas Injection (MGI) and provide redundancy and backup in case of SPI/MGI failure. Stabilization and suppression of post disruption RE beam has been tried on FTU, with a control architecture that allows to detect the current quench and to induce via the central solenoid a controlled RE beam current ramp-down meanwhile the beam is kept away from the vessel. The RE beam energy suppression is achieved, as confirmed by analyzing Hard X-ray (HXR) monitors and the Runaway Electron Imaging Spectroscopy (REIS) system, that measures the synchrotron radiation emitted by REs. In addiction, an estimation technique to retrieve the RE energy distribution function from REIS has been developed. The effectiveness of the proposed control scheme, tested also on TCV, has been discussed for ITER, where the control system should be able to maintain the RE beam for current quenches smaller than
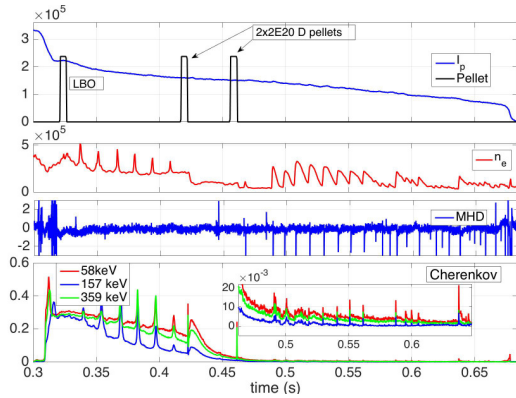
---

[*] See Appendix A

[**]See Appendix B

Figure 1. A post-disruption RE beam on which a first injection of iron with LBO followed by two deuterium pellets has been tested on a RE plateau. Electron density spikes are simultaneous to Cherenkov probe spikes, revealing that REs are expelled from the beam core due to instabilities. A fan-like instability take place after 0.45 s, whereas previous RE expulsions seems to have a different origin.

4 MA. Initial studies have revealed that fast changing electrical fields (via central solenoid and EC antenna) destabilize REs orbits, possibly inducing peculiar MHD instabilities growth (Figure 1). Different types of RE instabilities in presence of thermal and cold background plasmas have been analysed, and their correlation with toroidal electric field and density has been investigated. Deuterium pellet and heavy material injections, by means of Laser Blow Off (LBO) technique, have been performed into steady-state flat-top discharges with REs and on post disruption RE beams, and data from the fast scanning CO2-CO interferometer and spectroscopy diagnostics have been analyzed in order to study the dynamics of particle interaction with the RE beam and ionization to possibly extrapolate information for ITER predictions.
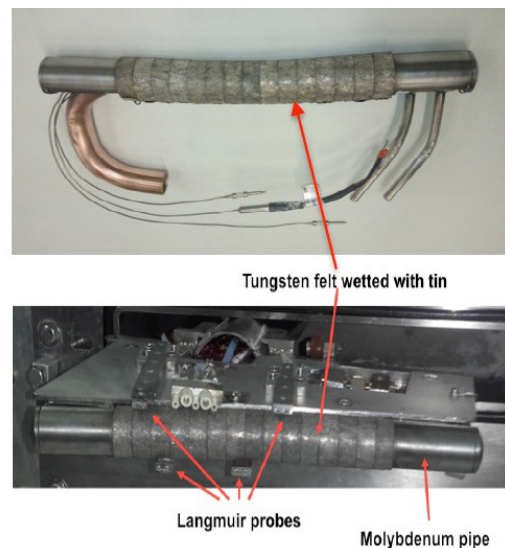
3. Tin Liquid Limiter experiments

In future fusion reactors, the divertor plates must not be subjected to average powers greater than 10 MW/m^2, with slow transients below 20 MW/m^2, and with an electron temperature below 5 eV. More than 90% of the power will be radiated in the center and/or in the Scrape-Off Layer (SOL), and the plasma will be partially detached. In this framework, liquid tin may prove a good candidate as a Plasma Facing Component (PFC) material, with a large operating window ($300 < T < 1300$ °C) before vaporization, low or negligible activation, and low H retention. Moreover, for $T > 1300$ °C, the thermal shield formed in front of the divertor plates by evaporated tin atoms can play an important role for power mitigation. Due to the high atomic number

Figure 2. Tin liquid limiter installed on FTU.

($Z = 50$), tin meets the high core radiation requirement, but the maximum tolerable tin concentration for DEMO should be less than 10^{-3} of the electron density to be sustainable [6]. The Tin Liquid Limiter (TLL) installed on FTU [7] (Figure 2) is based on the innovative concept of the Capillary Porous System (CPS) [8]. It consists of a molybdenum tube around which strips made of tungsten felt filled with tin are wrapped. To avoid hot spots in the intermediate region between strips, the TLL head was realized with a bending radius ($r_{TLL} = 129$ cm) in the poloidal direction, much greater than the minor radius of the plasma ($a = 29$ cm) in order to have a better and easier alignment of the CPS strips. The TLL can be

cooled by flowing air and atomized water in a copper pipe inserted inside the molybdenum tube. The TLL limiter is equipped with several thermocouples and four Langmuir probes, two on each side. The surface temperature of the TLL limiter is recorded with a fast Infrared (IR) camera observing the whole TLL surface from the top of the FTU machine ($\cong$ 1 mm of spatial resolution and up to 1200 frames/s of acquisition rate). A 2 m grazing incidence Schwob-Fraenkel XUV spectrometer [9] was installed on FTU observing the plasma emission in the range from 20 to 340 Å, to identify the spectral lines of Sn, with high spectral resolution. (Figure 3).

The TLL (without active cooling) was carefully tested with standard FTU pulses at toroidal magnetic field $B_T = 5.3$ T, plasma current $I_p = 0.5$ MA and flat-top duration of 1.3 sec, and the experimental results (obtained for the first time in the world in a tokamak with a TLL) have been carefully analyzed. The thermal load on the limiter was progressively varied moving up the limiter shot by shot into the SOL, until almost reaching the Last Closed Magnetic Surface (LCMS), and by increasing the electron density at fixed limiter radial position (the electron temperature in the SOL of the FTU standard discharge of approximately 20 eV is almost independent of electron density). The maximum heat flux deduced by the Langmuir probes was about 15 MW/m^2 for almost 1 s, for a TLL position closest to the LCMS. The maximum surface temperature measured by
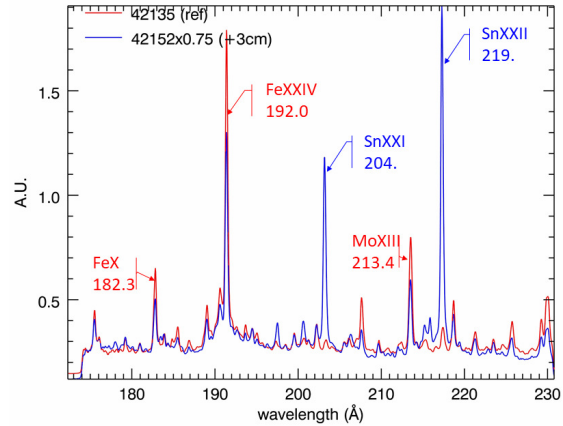

Figure 3. Comparison of one segment of the spectrum observed by the Schwob-Fraenkel XUV spectrometer for two discharges, one with the TLL fully retracted (in red), and the other with the TLL at +3 cm (in blue). The blue curve is normalized to the same background level.

the IR fast camera on the tin limiter was approximately 1700 °C, reached at the end of the pulse. These results have been satisfactorily reproduced with the 3D finite-element code ANSYS, with a deviation of the measured Sn surface temperature from the simulated one only at the end of the pulse, which could be due to the development of a tin cloud (vapour shield) near the TLL limiter. In particular, by looking at the temporal evolution of the IR maximum surface temperature and of the measured Sn XXI line emission monitored by the survey UV spectrometer SPRED, it was deduced that tin evaporation becomes the dominant tin production mechanism when the maximum surface temperature of the limiter exceeds 1300 °C. It is worth pointing out that no droplets have been observed entering into the plasma during the entire FTU experimental campaign and no damages were observed on the TLL after the plasma exposure. The effects on plasma performance were evaluated especially when tin evaporation was dominant. A concentration of tin of about 5×10^{-4} of the electron density was deduced from the variation of the Z_{eff} value [10], under the assumption that it was due entirely to tin. The JETTO code was used to compare two similar pulses with and without the tin limiter for the case in which tin evaporation was strong. The confinement time was practically the same within the error bars (10÷15%), without any degradation of the plasma performance.

4. Elongated plasmas

Preliminary experiments with elongated configurations were used on FTU to develop a proper elongation control [11]. Recently, a new vertical controller has been designed to stabilize vertically elongated plasmas in FTU, where Vertical Displacement Events (VDE) have been observed. In the latest experimental campaigns, experimental results showed its capability of stabilizing plasma up to the FTU record elongation of 1.23. As an example, a comparison between the standard Proportional-Integral-Derivative (PID) controller and the new hybrid controller is reported in Figure 4.
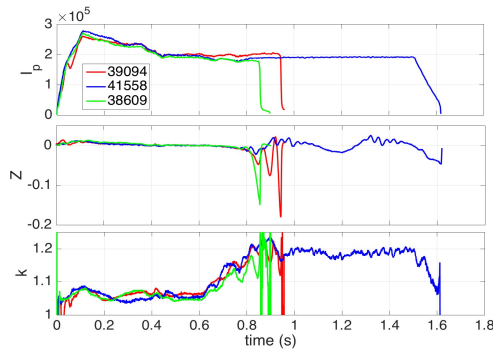

Figure 4. From top to bottom: plasma current I_P, vertical displacement z, and elongation k.

In the pulses #39094 (red) and #38609 (green) the standard PID controller is considered and the pulses have been vertically lost. On the contrary, when the hybrid controller has been introduced, the vertical confinement has been evidently improved as shown by the reported time traces (vertical displacement *z* and elongation *k*) of the pulse #41558 (blue). The parameters tuning required 3 pulses, which is few if considered to other type of controllers tuning. Further adaptive algorithms will be employed to extend control performances in case of long pulses.

Elongated plasmas pulses using the liquid metal limiters (lithium or tin) as primary limiter is the subject of on-going research.

5. Dust studies

Dust remobilization in tokamaks has been long recognized to be an issue affecting normal plasma operations. Evidence of the presence of an unexpected significant fraction of ferromagnetic dust in tokamak machines with both CFC and full-metal wall are reported in literature [12-14]. Magnetic dust particles, in contrast to non-magnetic ones, could be mobilized during, or even prior to, the discharge start-up, preventing a positive evolution or leading to an inhibition of plasma discharge. To date not enough attention has been paid to this type of events with studies exclusively focusing on dust remobilization only after full plasma pulse is established [15, 16]. Recent investigation on FTU proved the presence of dust mobilized prior to pulse start-up phase, when in the tokamak volume the magnetic field consists just of the time growing toroidal and multipole components due to the external coils. Evidence was provided by Thomson Scattering (TS) and IR camera diagnostics triggered before the beginning of pulses. In particular, TS spectra have shown the presence of dust in the chamber both before the ignition of the plasma pulse and during sole magnetic field time evolution pulses (i.e. no plasma ignition) routinely used for diagnostic zeroing. An estimation of dust concentration and size based on TS spectra and IR camera images indicated an average density of the order of 10^{-3} cm^{-3} and grains size between tens of μm and few mm. Taking into account all possible origin of these observations, the only plausible explanation is the remobilization of magnetic dust presents in FTU vessel, due to the force applied by the magnetic field. A study of possible impacts of mobilized magnetic dust on tokamak operations have led to the conclusion that dust flying during the early stages of the pulse build-up could interfere mainly in three ways: shifting the optimal loop-voltage vs. gas

pressure curve during breakdown phase (shift in the Paschen's curve), as consequence of reduced effective avalanche rate due to electron attachment to dust; perturbing the Z_{eff} and resistivity of plasma inducing a delay in the plasma ramp-up phase up to few 100s ms; inducing disruptions when the full plasma is established due to the evaporation of massive grains of high Z magnetic dust that could be present right in the plasma core. All the above three mechanisms depend on the actual dust density in the vessel.

6. Tearing Modes analysis with MARS code

A tearing mode is an instability that arises in magnetically confined plasma as a consequence of the plasma finite resistivity. It develops on q rational surfaces and it is driven by the radial gradient of the toroidal current density. A detailed study on tearing modes has been carried out in the contest of high density regimes, where the magnetic perturbation associated to the mode can increase up to disruption [17, 18]. When the density increases, an increase of the radiation losses is also observed which leads to contraction of the temperature profile and so to shrinkage of the current profile. Because the tearing mode is driven by the radial gradient of the current, as the current shrinks, tearing modes appear in the experimental pulse. The onset and the dynamics of the tearing modes during FTU pulses has been analyzed by means of the MARS code [19], which is a global, resistive, spectral code for full MHD linear stability analysis. To this aim, the temporal evolution of the pulse has been reconstructed from the experimental data with the JETTO transport code. The equilibria obtained at different times were then translated into the CPOs (Consistent Physical Objects) data environment, thus being suitable to be read by a high-resolution equilibrium code solver such as CHEASE [20]. Indeed, it is worth noting that both the CHEASE code and the MARS code are fully compliant with the WPCD CPOs environment and, recently, they have been ported to the IMAS environment as well.
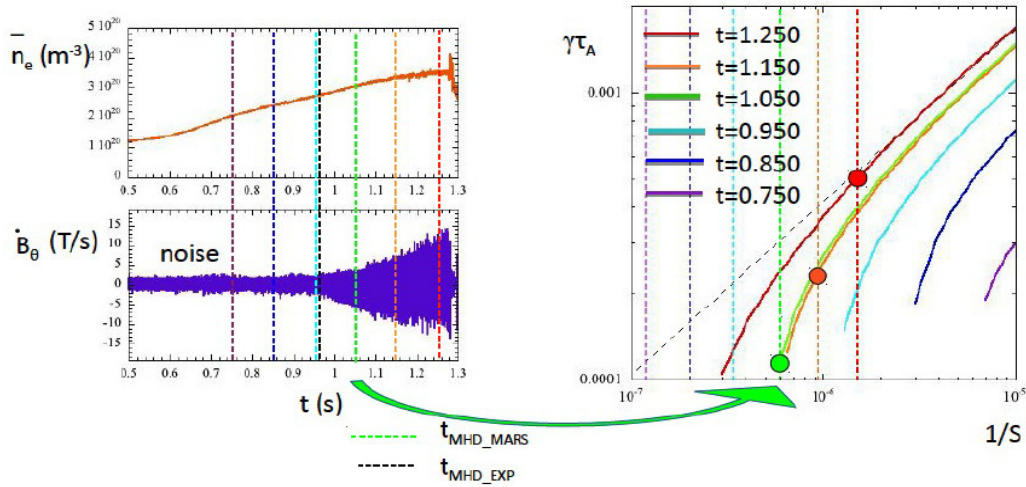

Figure 5. FTU pulse #34769. $B_T = 8$ T, $I_p = 900$ kA. (Left) Line density and perturbed poloidal magnetic field evolution. (Right) MARS output for different times (equilibria) during the density ramp-up. The effective values of the experimental inverse Lundquist number in FTU are shown as vertical dotted lines.

The dynamics of a sufficient number of FTU pulses has been analyzed in the high density regimes with different plasma current I_p (500 kA up to 900 kA) and different toroidal magnetic field B_T (4 T up to 8 T). The onset of the tearing mode, established by the MARS code simulations, has been compared with the one observed experimentally from pick-up coil signals and a good agreement can be claimed. In Figure 5 it is shown, as an example, one

single shot analyzed (#34769). On the left hand side the experimental evolution of the line density profile and the temporal evolution of the perturbed poloidal magnetic field are shown; on the right hand side the growth rate (normalized to the Alfvén time) of the mode for different times (0.75 s up to 1.25 s), and thus different equilibria, is shown as a function of the inverse Lundquist number *1/S*. Vertical lines represent the experimental inverse Lundquist number in FTU at a certain time; of course, if the vertical line intercepts the growth rate curve, the mode is unstable, viceversa it is stable. In the figure, instability is observed for a time greater equal than 1.05 s (green dotted line), which can be compared to the experimental onset found around 1.00 s (black dotted line). Note that the curve bending of the growth rate is due to curvature effect; indeed, additional simulations have been performed with MARS progressively reducing the plasma pressure: in this case, besides increasing the growth rate at high *1/S* values, also the curve bending at low *1/S* values disappears and the mode always results unstable in the considered time window. Finally, MARS results have been validated with convergences test on the mesh size, the number of spectral components and the mesh packaging around the rational *q* surfaces.

7. Highly collisional regimes

In literature an inverse linearity between the electron density peaking and the effective collisionality ν_{eff} is found for most tokamaks devices [21], as reported in Figure 6 for pulses with ν_{eff} from 0.2 to 10 (grey symbols). FTU offers the unique opportunity to explore regimes of high collisionality (up to ~ 100), thanks to the capability to operate up to very high electron density values. It has been observed that the inverse linearity of the density peaking versus the effective collisionality is similar to other devices at low and medium collisionality (JET, Asdex, JT-60U, and Alcator C-mod, although in H-mode regime). However, at high values of the collisionality such inverse linearity does not occur, but, instead, an increase of the density peaking with the collisionality is
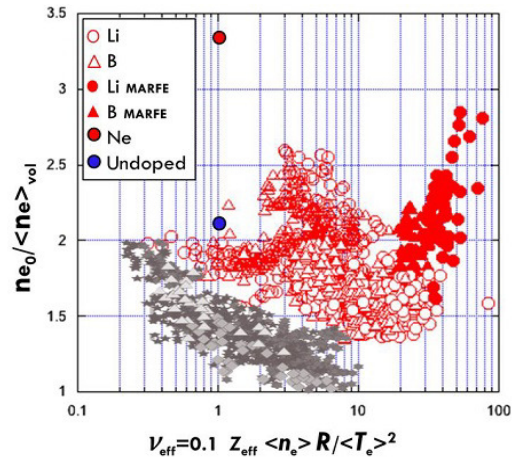

Figure 6. Density peaking as a function the effective collisionality. Red symbols for FTU data; grey symbols for other devices. The behaviour of a Ne doped pulse on FTU is also reported.

found, as reported in Figure 6 (red symbols). In particular, from the comparison between pulses with and without the MARFE instability and with Li or B wall conditioning, it seems that the increase of the density peaking is related to an edge phenomenon, as the MARFE instability presence and ameliorated conditioning of wall by using the lithium limiter [22]. In these cases, plasmas of particular interest in terms of density peaking [17] are observed. Another interesting effect is associated to the Neon injection [23]: keeping the same collisionality, an impressive increase of the density peaking is obtained for doped pulses with respect to the un-doped ones.

8. Diagnostics

Runaway Electron Imaging Spectroscopy (REIS). The REIS system, developed to detect images and spectra of synchrotron emission from in-flight REs, was calibrated and commissioned as a portable diagnostic for operation in medium sized tokamak. First operated in FTU, after design and construction of suitable interfaces, the REIS was installed in AUG and TCV and exploited in RE generation and control experiments. The REIS system is a wide-angle optical diagnostics collecting RE synchrotron radiation from two plasma cross sections (corresponding to RE backward and forward views) and transmitting it to visible/infrared spectrometers via an incoherent bundle of fibres. The present operating spectral range spans from 0.3 to 2.5 μm, and it will be extended to 5 μm in a major re-design and upgrade in 2018. As an example of the information provided by the REIS diagnostics, for FTU pulse #39516, in which REs are generated already in the very early

Figure 7. Pulse #39516. Visible camera images of the RE beam (left): the bottom image (corresponding to frame 013255, t = 0.4 s) shows both RE backward and forward views, while the top image is a time sequence of the forward view for the same pulse. Note the temporal correlation of the visible images with the measured synchrotron radiation intensity at several wavelengths (right top) and synchrotron radiation visible spectra (right bottom): the spectra are fitted (solid lines) assuming mono-energetic distributions (energy and pitch angle values in the insert).

stages of the pulse, in Figure 7 are shown images of the RE beam from the visible camera (left) correlated with the measured synchrotron radiation intensity at several wavelengths (right top) and the measured synchrotron radiation visible spectra (right bottom). The spectra are fitted (black solid lines) using formula (1) from [24] for a mono-energetic RE distribution. It is worth noting that the measured energy and pitch angle values (see insert in Figure 7, right bottom) are in agreement with the predictions of simulations based on a test particle model of the RE dynamics [25]: the calculated RE energy distribution gradually becomes mono-energetic with a maximum energy of ~ 30 MeV.

Cherenkov probe. Predicting and controlling plasma disruptions in tokamaks is one of the key features for a reliable application of nuclear fusion. In particular, measurements of fast electrons produced in the plasma core and escaping from it are of interest to study processes occurring inside the plasma itself. Cherenkov diagnostic is a good candidate to perform these studies and both single and triple Cherenkov probes were installed on FTU and their performances have been under investigation [26]. In particular, the triple probe differs from the single one for the fact that it has three diamond detectors with three different energy thresholds (58, 187 and 359 keV), thus it is able to perform a first energy scan. Each diamond detector is mounted on a Titanium Zirconium Molybdenum (TZM) head inserted into the FTU vessel, and it is coated with a Ti/Pt/Au interlayer filtering out visible light, particularly the plasma D_α line. In the triple probe, two of them have a further deposition of Mo, respectively 56 μm and 164 μm in order to have different threshold energies. Electrons impinging on the probe emit Cherenkov radiation in diamond, and this radiation is routed, through a visible/ultraviolet optical fibre, to a PMT operating at high voltage (1 kV) with a detectable range of 185÷850 nm. An example of analysis focuses on the capability and sensitivity of the probes to measure runaway electrons losses with energy discrimination in presence of
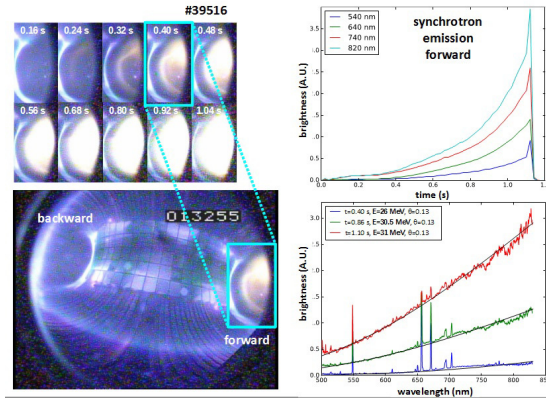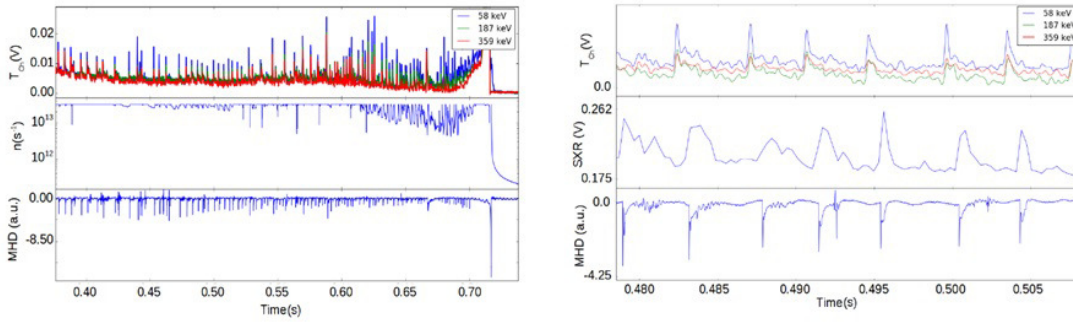
Figure 8. (Left) Correlation between triple Cherenkov probe signal, gamma-ray count rate and MHD activity. (Right) Triple Cherenkov signal, Soft X-rays and MHD activity. Pulse #41146.

perturbations due to kinetic reconnection phenomena is described in the following, confirming the Cherenkov probe to be a valid diagnostic system to study and monitor plasma scenarios involving REs generation. Anomalous Doppler Effect (ADE), also known as Fan instability, is a kinetic instability that tends to transfer energy from parallel (with respect to magnetic field *B*) to perpendicular particle motion. Figure 8 (left) shows an example, with comparison between Cherenkov signals, gamma-ray emission rate and magnetic activity. During plasma pulse #41146 REs expulsion due to the ADE appeared in the ramp-down phase driven by a Soft-Stop (active control activates when a safety threshold value on Hard X-rays signal is exceeded for more than 10 ms). The most notable thing is the correlation of each peak from X-rays and Cherenkov signals to those from the MHD activity, also visible on a smaller scale on Figure 8 (right). At this time scale, it is seen that these peaks rapidly rise up in just a few μs. Note, moreover, that the Cherenkov peaks are clean and more distinct than those from the X-ray signals, due to the better time resolution of the probes. Regarding the thresholds, the blue signal dominates (58 keV), followed by the green (187 keV) and the red one (359 keV). This shows that, during this discharge, Fan instability generates expulsion of REs with energies in general smaller than those usually observed.

Collective Thomson Scattering (CTS) diagnostics. The CTS diagnostic allows the investigation of ion populations in fusion plasma devices, studying the characteristic emissions, stimulated by the injection of a powerful microwave probing beam. From the shape of the emitted spectrum, plasma parameters such as ion temperature, drift velocity and ion composition can be inferred [27, 28]. The availability in FTU of a CTS diagnostic system at 140 GHz and the possibility of "non-resonant" plasma scenarios, i.e. scenarios in which the Electron Cyclotron (EC) layer (and harmonics) resonant with the probe frequency are out of the plasma region, allow carrying out studies on ions characteristics. In fact, in presence of EC resonances, the Electron Cyclotron Emission (ECE) background (at probing frequency) can significantly overwhelm the signals due to thermal CTS. Nevertheless, in recent experiments, the CTS diagnostics was used also for investigations on Parametric Decay Instability excitation by EC beams in correlation with magnetic islands induced by neon injection and in resonant scenarios [29]. Parasitic emissions from the gyrotron were observed, while other spectral emissions (lines and bands) have been observed and analyzed with very high time and frequency resolution. To determine the emissions mechanism and locate the plasma volume originating them, an independent receiving line has been recently installed.

Laser Induced Breakdown Spectroscopy (LIBS). The quantitative detection of tritium retained in the ITER in vessel components is mandatory for deciding if the machine operation must be stopped and the exceeding tritium removed. Laser Induced Breakdown Spectroscopy

is a suitable not invasive in situ diagnostic for detecting retained tritium; in particular, the Multi-Purpose Deployer, a robotic arm which can be installed on ITER during maintenance, could be equipped with LIBS system to analyze a consistent area of the vessel. In the last year, LIBS measurements of the deuterium (used as a proxy for tritium) retained in and the surface elemental composition of the FTU Mo (TZM) toroidal limiter tiles, have been carried out from remote (~ 2.5 m) during machine maintenance [30], with measurements performed both in vacuum and in Nitrogen or Argon atmosphere. The main goal of the experiments was to verify the feasibility of retained deuterium detection for supporting the proposed use of a robotic arm for an extended LIBS analysis of the in vessel FTU components.

The experimental layout consisted of a Quantel laser "Twin BSL" (λ = 1064 nm), a Andor "Istar DH320T-18F-63" ICCD camera with 1024x512 sensor (26 μm pixels) and a Jobin Ivon "Triax 550" spectrometer (550 mm) with 2400 grooves/mm grating. Single pulse technique has been used. The collinear transmission of the laser beam and detection of emitted visible lines was done through the 2 inches window of an equatorial port by using a dielectric mirror. Laser and optics for laser transmission and visible lines detection were mounted on a plate movable along three axes and able to be pivoted. Vacuum measurements resulted in a good resolution of D_α and H_α emission lines (Figure 9) and in
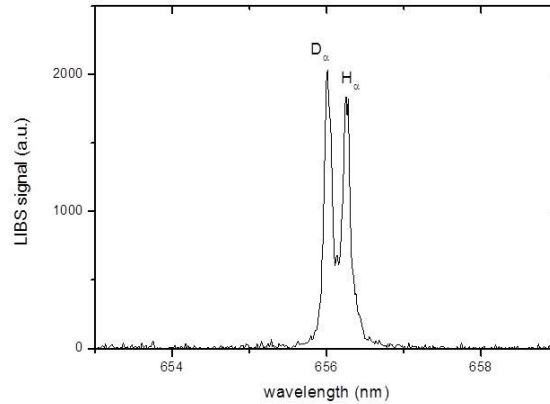

Figure 9. Deuterium and Hydrogen emission lines detected by LIBS on a shadowed zone in between the FTU toroidal limiter tiles.

the detection, besides Mo, the main component of the TZM alloy, of Li coming from the lithium deposited during the experiments with lithium limiter, inserted in the vessel through a vertical port located 60° toroidally apart. Deuterium was also detected in shadowed zones in between tiles. Measurements carried out at atmospheric pressure showed different results depending on the used gas, Nitrogen or Argon. With Nitrogen (1000 mbar) no evident deuterium and hydrogen emission lines were detected. The limited available experimental time did not allow a deep analysis of the causes: a possible explanation is the partial formation of NH and ND compounds, of which the emission lines in the LIBS plasma plume were not detectable in our experiments given the cut of emitted line wavelengths below 400 nm, caused by the dielectric mirror. With Argon atmosphere (500 mbar) the deuterium and hydrogen emission lines were well visible although with worse resolution with respect to vacuum measurements, as it was to be expected because of the larger Stark broadening of emitted lines. After a fresh boronization (routinely performed in FTU by using deuterated diborane) deuterium was also detected together with Boron lines, therefore reproducing, at least partially, the ITER situation, where tritium is foreseen to be retained in the machine mainly by co-deposition with beryllium.

9. Conclusions

LIBS measurements of the deuterium retained on the FTU Mo toroidal limiter tiles have shown that LIBS is a suitable not invasive in situ diagnostic for a quantitative detection of tritium retained in the ITER vessel components. Recent investigation on FTU proved the presence of dust mobilized prior to pulse start-up phase, when in the tokamak volume the

magnetic field consists just of the time growing toroidal and multipole components due to the external coils. Stabilization and suppression of post disruption RE beam has been achieved on FTU, with a control architecture that allows to detect the current quench and to induce via the central solenoid a controlled RE beam current ramp-down meanwhile the beam is kept away from the vessel. The REIS diagnostic has allowed to provide simultaneously the image and the visible/infrared spectrum of the forward and backward radiation from in flight REs. The Tin Liquid Limiter was tested with standard FTU pulses (B_T = 5.3 T, I_p = 0.5 MA); the maximum thermal load deduced by the Langmuir probes was about 15 MW/m^2 for almost 1 s, without any degradation of the plasma performance, proving liquid tin to be a good candidate as a Plasma Facing Components material. A 2 m grazing incidence Schwob-Fraenkel XUV spectrometer was installed on FTU observing the plasma emission in the range from 20 to 340 Å, to identify the spectral lines of Sn, with high spectral resolution, during the TLL experiments. A new vertical controller has been designed to stabilize vertically elongated plasmas in FTU, where Vertical Displacement Events have been observed. Experimental results showed its capability of stabilizing plasma up to the FTU record elongation of 1.23. The onset of TMs in the high density regime has been analyzed by means of the MARS code, which is a global, resistive, spectral code for full MHD linear stability analysis. The obtained onset times have been compared with the ones observed experimentally from pick-up coil signals and a good agreement can be claimed. An increase of the density peaking with the effective collisionality ν_{eff} has been found on FTU at high values of ν_{eff}. This behavior seems to be related to an edge phenomenon, as the MARFE instability presence and ameliorated conditioning of wall by using the Li limiter. The CTS diagnostics was used for investigations on Parametric Decay Instability excitation by EC beams in correlation with magnetic islands induced by neon injection. Parasitic emissions from the gyrotron were observed, while other spectral emissions have been observed and analyzed. A triple Cherenkov probe was installed and tested on FTU, confirming the Cherenkov prove to be a valid diagnostic system to study and monitor plasma scenarios involving REs.

References

[1]   GORMEZANO, C., DE MARCO, F., MAZZITELLI, G., et al., "The FTU program", Fusion Sci. Technol. **45** (2004) 297.

[2]   SAINT-LAURENT, F., et al., "Control of Runaway Electron Beam Heat Loads on Tore Supra", Proc. 38th EPS Conf. on Plasma Physics (Strasbourg, France, 2011) **O3.118**.

[3]   HOLLMANN, E. M., et al., "Control and dissipation of runaway electron beams created during rapid shutdown experiments in DIII-D", Nucl. Fusion **53** (2013) 083004.

[4]   ESPOSITO, B., et al, "Runaway electron generation and control", Plasma Phys. Control. Fus. **59** (2017) 014044.

[5]   CARNEVALE, D., et al., "Active control for current dissipation of runaway electrons in TCV", Proc. 44th EPS Conf. On Plasma Physics (Belfast, Northern Ireland 2017), **P1.152**.

[6]   PORADZINSKI, M., et al., "Integrated core-SOL-divertor modelling for DEMO with tin divertor", Fusion Eng. Des. **124** (2017) 248.

[7]   VERTKOV, A., et al., "Liquid Tin Limiter for FTU tokamak", Fusion Eng. Des. **117** (2017) 130.

[8]   VERTKOV, A., et al., "Technological aspects of liquid lithium limiter experiment on FTU tokamak", Fusion Eng. Des. **82** (2007) 1627.

[9]   SCHWOB, J. L., et al., "High-resolution duo-multichannel soft x-ray spectrometer for tokamak plasma diagnostics", Rev. Sci. Instrum. **58** (1987) 1601.

[10]   BOMBARDA, F., et al., "High Resolution EUV Spectroscopy on FTU with Tin Liquid Limiter", 45th EPS Conf. on Plasma Physics (Prague, Czech Republic, 2018), **P1.1005**.

[11]   RAMOGIDA, G., CALABRO′ G., et al., "D-shaped configurations in FTU for testing liquid lithium limiter: Preliminary studies and experiments", Nucl. Mat. Energy **12** (2017) 1082.

[12]   IVANOVA, D., RUBEL, M., PHILIPPS, V., et al., "Survey of dust formed in the TEXTOR tokamak: structure and fuel retention", Phys. Scr. **T138** (2009) 014025.

[13]   NOVOKHATSKY, A. N., GORODETSKY, A. E., GUSEV, V. K., et al., "Structure and chemical composition of magnetic dust formed in Globus-M tokamak", Proc. 38th EPS Conf. on Plasma Physics (Strasbourg, France, 2011) **P5.066**.

[14]   DE ANGELI, M., LAGUARDIA, L., MADDALUNO, G., et al., "Investigation on FTU dust and on the origin of ferromagnetic and lithiated grains", Nucl. Fusion **55** (2015) 123005.

[15]   TOLIAS, P., RATYNSKAIA, S., DE ANGELI, M., et al., "Dust remobilization in fusion plasmas under steady state conditions", Plasma Phys. Control. Fusion **58** (2016) 025009.

[16]   RATYNSKAIA, S., TOLIAS, P., BYKOV, I., et al., "Interaction of adhered metallic dust with transient plasma heat loads", Nucl. Fusion **56** (2016) 066010.

[17]   PUCELLA, G., TUDISCO, O., et al., "Density limit experiments on FTU", Nucl. Fusion **53** (2013) 083002.

[18]   PUCELLA, G., et al., "Development of magnetic island near the density limit on FTU", Proc. 40th EPS Conf. on Plasma Physics (Espoo, Finland, 2013) **P5.139**.

[19]   BONDESON, A., VLAD, G., and LUTJENS, H., "Resistive toroidal stability of internal kink modes in circular and shaped tokamaks", Phys. Fluids B **4** (1992) 1889.

[20]   LUTJENS, H., BONDESON, A., SAUTER, O., "The CHEASE code for toroidal MHD equilibria", Comput. Phys. Commun. **97** (1996) 219.

[21]   ANGIONI, C., et al., "Particle transport in tokamak plasmas, theory and experiment", Plasma Phys. Control. Fus. **51** (2009) 124017.

[22]   MAZZITELLI, G., APICELLA, M. L., et al., "FTU results with a liquid lithium limiter", Nucl. Fusion **51** (2011) 073006.

[23]   MAZZOTTA, C., et al., "Peaked density profiles due to neon injection on FTU", Nucl. Fusion **55** (2015) 073027.

[24]   STAHL, A., et al., "Synchrotron radiation from a runaway electron distribution in tokamaks", Phys. Plasmas **20** (2013) 093302.

[25]   POPOVIC, Z., et al., "On the measurement of the threshold electric field for runaway electron generation in the Frascati Tokamak Upgrade", Phys. Plasmas **23** (2016) 122501.

[26]   CAUSA, F., et al., "Cherenkov emission provides detailed picture of non-thermal electron dynamics in the presence of magnetic islands", Nucl. Fusion **55** (2015) 123021.

[27]   STEJNER, M., et al., "Plasma rotation and ion temperature measurements by collective Thomson scattering at ASDEX Upgrade", Plasma Phys. Control. Fusion **57** (2015) 062001.

[28]   STEJNER, M., et al., "Principles of fuel ion ratio measurements in fusion plasmas by collective Thomson scattering", Plasma Phys. Control. Fusion **53** (2011) 065020.

[29]   BRUSCHI, A., et al., "Observation of short time-scale spectral emissions at millimeter wavelengths with the new CTS diagnostic on the FTU tokamak", Nucl. Fusion **57** (2017) 076004.

[30]   MADDALUNO, G., et al., "Detection by LIBS of the deuterium retained in the FTU toroidal limiter", 23rd PSI Conference (Princeton, USA, 2018), abstract number **391**.

Appendix A: Members of the FTU Team

E. Alessi[2], B. Angelini[1], M. L. Apicella[1], G. Apruzzese[1], G. Artaserse[1], B. Baiocchi[2], F. Belli[1], W. Bin[2], F. Bombarda[1], L. Boncagni[1], A. Botrugno[1], S. Briguglio[1], A. Bruschi[2], P. Buratti[1], G. Calabrò[1], M. Cappelli[1], A. Cardinali[1], D. Carnevale[3], L. Carraro[4], C. Castaldo[1], F. Causa[2], S. Ceccuzzi[1], C. Centioli[1], R. Cesario[1], C. Cianfarani[1], G. Claps[1], V. Cocilovo[1], F. Cordella[1], F. Crisanti[1], O. D'Arcangelo[1], M. De Angeli[2], C. Di Troia[1], B. Esposito[1], F. Fanale[2], D. Farina[2], L. Figini[2], G. Fogaccia[1], D. Frigione[1], V. Fusco[1], L. Gabellieri[1], S. Garavaglia[2], E. Giovannozzi[1], G. Gittini[2], G. Granucci[2], G. Grosso[2], M. Iafrati[1], F. Iannone[1], L. Laguardia[2], E. Lazzaro[2], M. Lontano[2], G. Maddaluno[1], S. Magagnino[1], M. Marinucci[1], D. Marocco[1], G. Mazzitelli[1], C. Mazzotta[1], V. Mellera[2], A. Milovanov[1], D. Minelli[2], F. C. Mirizzi[5], A. Moro[2], S. Nowak[2], D. Pacella[1], F. Pallotta[2], L. Panaccione[5], M. Panella[5], V. Pericoli-Ridolfini[5], A. Pizzuto[1], S. Podda[1], G. Pucella[1], M. E. Puiatti[4], G. Ramogida[1], G. Ravera[1], D. Ricci[2], A. Romano[1], A. Simonetto[2], C. Sozzi[2], U. Tartari[2], A. A. Tuccillo[1], O. Tudisco[1], M. Valisa[4], B. Viola[1], E. Vitale[1], G. Vlad[1], B. Zeniol[4], M. Zerbini[1], F. Zonca[1], M. Aquilini[1], P. Cefali[1], E. Di Ferdinando[1], S. Di Giovenale[1], G. Giacomi[1], A. Grosso[1], M. Mezzacappa[1], A. Pensa[1], P. Petrolini[1], V. Piergotti[1], B. Raspante[1], G. Rocchi[1], A. Sibio[1], B. Tilia[1], R. Tulli[1], M. Vellucci[1], D. Zannetti[1].

[1]ENEA, Fusion and Nuclear Safety Department, C.R. Frascati, Via E. Fermi 45, 00044 Frascati (Roma), Italy
[2]Istituto di Fisica del Plasma, Consiglio Nazionale delle Ricerche, Via R. Cozzi 53, 20125 Milano, Italy
[3]Università di Roma Tor Vergata, Dipartimento di Ingegneria Civile e Informatica, Viale del Policlinico 1, 00133 Roma, Italy
[4]Consorzio RFX, Corso Stati Uniti 4, 35137, Padova, Italy
[5]Consorzio CREATE, Università di Napoli Federico II, Via Claudio 21, 80125 Napoli, Italy

Appendix B: Collaborators

S. Almaviva[1], F. Bagnato[6], G. Brolatti[1], A. Buscarino[7], L. Calacci[3], L. Caneve[1], M. Carlini[8], F. Colao[1], C. Corradino[7], P. Costa[1], F. Crescenzi[1], A. Cucchiaro[1], A. Doria[1], G. Ferrò[3], A. Gabrielli[3], S. Galeani[3], C. Galperti[6], P. Gasior[9], E. Giovenale[1], M. Gospodarczyk[3], L. Jakubowski[10], M. Kubkowska[9], A. Lampasi[1], V. Lazic[1], L. Lubyako[11], G. Maffia[1], F. Martinelli[3], J. R. Martin-Solis[12], F. Maviglia[5], R. Mazzuca[1], M. Moneti[8], F. P. Orsitto[5], A. Palucci[1], M. Passeri[3], Z. Popovic[12], C. Possieri[3], M. Rabinski[10], S. Ratynskaia[13], M. Reale[1], S. Roccella[1], M. Sassano[3], F. Starace[1], P. Tolias[13], A. Vertkov[14], J. Zebrowski[10], P. Zito[1].

[1]ENEA, Fusion and Nuclear Safety Department, C.R. Frascati, Via E. Fermi 45, 00044 Frascati (Roma), Italy
[3]Università di Roma Tor Vergata, Dipartimento di Ingegneria Civile e Informatica, Viale del Policlinico 1, 00133 Roma, Italy
[5]Consorzio CREATE, Università di Napoli Federico II, Via Claudio 21, 80125 Napoli, Italy
[6]Ecole Polytechnique Fédérale de Lausanne, Swiss Plasma Centre, CH-1015 Lausanne, Switzerland
[7]Università di Catania, Department of Electrical, Electronics and Computer Engineering, Catania, Italy
[8]Università della Tuscia, Centre for Research and Dissemination of Renewable Energy, 01028 Orte, Italy
[9]Institute of Plasma Physics and Laser Microfusion, Warsaw, Poland
[10]National Centre for Nuclear Research, 7 Andrzeja Soltana Str., 05-400 Otwock, Poland
[11]Institute of Applied Physics, 46 Ulyanov st., Nizhny Novgorod, 603950, Russian Federation
[12]Universidad Carlos III de Madrid, Avenida de la Universidad 30, 28911 Madrid, Spain
[13]Space and Plasma Physics - KTH Royal Institute of Technology, SE-10044, Stockholm, Sweden
[14]JSC Red Star, Moscow, Russian Federation